Reverse Micelles Dissolved in Supercritical Xenon: An NMR Spectroscopic Study

Matthias Meier, Alexander Fink, and Eike Brunner*

Institute of Biophysics and Physical Biochemistry, University of Regensburg, D-93040 Regensburg, Germany

Received: November 9, 2004; In Final Form: December 10, 2004

Reverse micelles currently gain increasing interest in chemical technology. They also become important in biomolecular NMR due to their ability to host biomolecules such as proteins. In the present paper, a procedure for the preparation of high-pressure NMR samples containing reverse micelles dissolved in supercritical xenon is presented. These reverse micelles are formed by sodium bis(2-ethylhexyl) sulfosuccinate (AOT). For the first time, NMR spectroscopy could be applied to reverse micelles in supercritical xenon. The AOT/H_2O/Xe system was studied as a function of experimental parameters such as xenon pressure, water content, and salt concentration. Optimum conditions for reverse micelle formation in supercritical xenon could be determined. It is, furthermore, demonstrated that biomolecules such as amino acids and proteins can be incorporated into the reverse micelles dissolved in supercritical xenon.

Introduction

Because of their unique properties, reverse micelles currently gain increasing interest in chemical technology.[1] Reverse micelles are nanometer-sized droplets of an aqueous solution stabilized in an unpolar solvent by surfactant molecules located at the interface.[2] Proteins can be incorporated into the aqueous core of such a microdroplet,[3−6] thus being protected from denaturation. Therefore, reverse micelles also become important in biomolecular NMR.[7−12] It is well-known that proteins with a molecular weight exceeding ca. 20 kDa dissolved in water exhibit relatively broad lines, an effect which limits the resolution in liquid-state NMR spectroscopic experiments.[13] Transverse relaxation optimized spectroscopy (TROSY) has significantly contributed to overcome this limitation.[14,15] Alternatively, Wand et al. have suggested to make use of reverse micelles to dissolve proteins in unpolar solvents such as liquid alkanes.[7,8] Although there are many different surfactants capable of forming reverse micelles and hosting proteins,[16] bis(2-ethylhexyl) sulfosuccinate[11,17] (AOT) is most often used for this purpose. Following the commonly used convention, the water content of the micellar solution is expressed by the ratio between the water concentration, $c(H_2O)$, and the surfactant concentration, c(AOT)

$$w_0 = \frac{c(H_2O)}{c(\mathrm{AOT})} \tag{1}$$

The correlation time, τ_C, of a spherical particle dissolved in a solvent of viscosity η can be described by the Stokes−Einstein relation

$$\tau_C = \frac{4\pi\eta r^3}{3kT} \tag{2}$$

where k is the Boltzmann constant, r the hydrodynamic radius of the considered particle, and T the absolute temperature. The line width observed for the dissolved particles is determined by the transverse relaxation time, T_2, which is governed by τ_C (see eq 3, below). Nonpolar solvents typically exhibit a lower viscosity than water (see Figure 1) which would result in a decrease of τ_C, i.e., narrower lines for particles dissolved in the low-viscosity solvents. Supercritical fluids such as ethane, CO_2, or xenon are particularly promising because of their very low viscosities. However, biomolecules such as proteins are usually insoluble in such solvents. For this reason, biomolecules have to be incorporated into a reverse micelle, which can be dissolved in a nonpolar solvent. It is important to note that the incorporation of a biomolecule into a reverse micelle results in an increased hydrodynamic radius, r, which means an increase of τ_C (see eq 2). The advantage of low-viscosity solvents is, therefore, abolished by the increase of r at least for smaller proteins. For larger proteins with a molecular weight exceeding

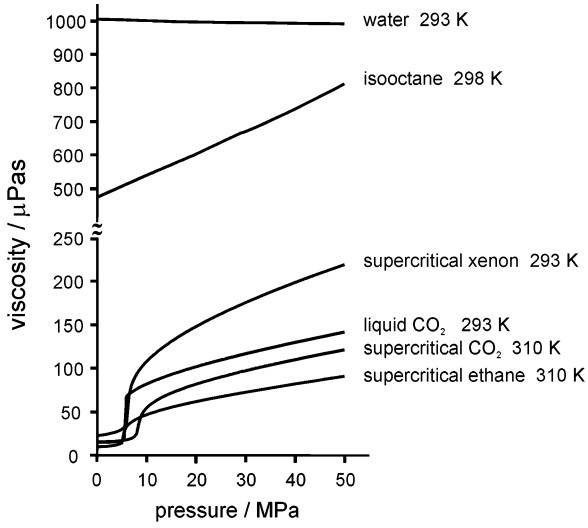

Figure 1. Viscosities of water and several unpolar solvents as a function of pressure. Data were taken from the National Institutes of Standards database (http://webbook.nist.gov/chemistry/fluid/). The critical temperatures, T_{crit}, pressures, p_{crit}, and concentrations, c_{crit}, are: xenon, $T_{crit} = 289.73$ K, $p_{crit} = 5.84$ MPa, $c_{crit} = 8.37$ mol/L; carbon dioxide, $T_{crit} = 304.13$ K, $p_{crit} = 7.38$ MPa, $c_{crit} = 10.63$ mol/L; ethane, $T_{crit} = 305.33$ K, $p_{crit} = 4.87$ MPa, $c_{crit} = 6.87$ mol/L.

* Author to whom corrrespondence may be addressed. Phone: +49 941 943 2492. Fax: +49 941 943 2479. E-mail: eike.brunner@biologie.uni-regensburg.de.

10.1021/jp044863g CCC: $30.25
Published on Web 01/28/2005

ca. 20 kDa, however, the situation changes. An estimation for such proteins shows that τ_C becomes shorter for the molecule hosted by a reverse micelle in the supercritical fluid compared to the molecule dissolved in water. With respect to viscosity, supercritical ethane is the best choice (see Figure 1). Xenon is, however, of special interest from the NMR spectroscopic point of view. ^{129}Xe, a spin-$^1/_2$ nucleus, can be hyperpolarized via spin-exchange optical pumping. It is also possible to transfer hyperpolarized ^{129}Xe into the supercritical state.[18] This methodology offers the opportunity of signal enhancement for molecules dissolved in supercritical xenon[19] by the so-called spin-polarization-induced nuclear Overhauser effect (SPINOE).[20] Reverse micelles formed by AOT in supercritical xenon were prepared and studied by dynamic light scattering for the first time by Fulton et al.[21,22] So far, NMR spectroscopic investigations have not been carried out on this system. The aim of the present paper is the extended NMR spectroscopic study of reverse micelles formed by AOT in supercritical xenon as well as investigations concerning the incorporation of biomolecules into these reverse micelles.

Experimental Section

All experiments were performed using a high pressure (HP) NMR apparatus[23] equipped with a sapphire tube (Saphikon, USA) which safely allows measurements up to 60 MPa (maximum pressures up to 100 MPa could be obtained). The xenon pressure within the tube was adjusted by a volumetric procedure. Pressures corresponding to the adjusted xenon densities were taken from the database of the National Institute of Standards, USA (http://webbook.nist.gov/chemistry/fluid/). Pressure values could be determined with an accuracy of ±3%.

Micellar solutions without guest molecules were prepared by placing purified[24] AOT (Fluka, Munich) and the corresponding amount of water at the bottom of the HP NMR tube before condensing the xenon into the tube. Unless specifically noted, the water contained 50 mM sodium acetate and 250 mM sodium chloride. These salt concentrations turned out to be optimum values as is described below. All samples were optically clear after homogenization by ultrasound treatment and equilibration for 1 day at room temperature. The real water content, w_0, of the micelles could be calculated from the ^{1}H NMR spectra using the intensity of the water signal and of the signal due to the CH_3 groups of the AOT molecules. An accuracy of ±10% could be estimated for the thus-determined real w_0 values. The real w_0 values were often found to be smaller than the "theoretical" values, w_0^{th}, expected from the amount of water used in the sample preparation. This observation shows that the water was not completely incorporated into the micelles in many cases.

The biomolecules to be inserted into the reverse micelles were first dissolved in water and then placed at the bottom of the HP NMR tube together with AOT before condensing the xenon into the tube. ^{15}N/^{13}C$^{\alpha}$ labeled glycine was purchased from Eurisotop (Saarbrücken, Germany). Lysozyme (Hybaid-AGS, Heidelberg, Germany), immunoglobuline G (Sigma-Aldrich), and trypsin (Roche Molecular Biochemicals, Mannheim, Germany) were also used.

^{1}H NMR measurements were performed on a Bruker DMX 500 spectrometer at 298 K. Chemical shifts were referenced using tetramethylsilane as an external standard. The accuracy for ^{1}H NMR chemical shift measurements was ±0.05 ppm. Transverse relaxation times, T_2, could be measured by standard Carr−Purcell−Meiboom−Gill (CPMG) experiments and longitudinal relaxation times, T_1, by inversion−recovery experiments. Pulsed-field gradient (PFG) experiments[25] were performed in order to identify and suppress the signals due to monomeric molecules in the samples. The maximum applied gradient strength was 5.3 mT/cm (100%); gradient pulses of 2.5 ms length and a delay of 75 ms were used. ^{1}H/^{13}C heteronuclear single quantum coherence (HSQC) correlation spectra were recorded using the standard HSQC pulse scheme.[26]

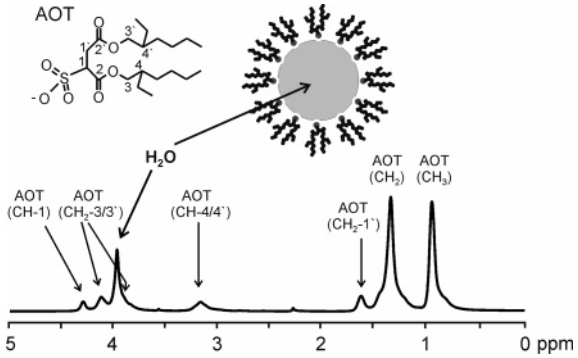

Figure 2. ^{1}H NMR spectrum of reverse micelles formed by 50 mM AOT in supercritical xenon at 15 MPa and $w_0^{th} = 6$. The aqueous solution used for the sample preparation contained 50 mM potassium phosphate (pH 5.5) and 250 mM sodium chloride.

Results and Discussion

^{1}H NMR and ^{1}H PFG NMR Spectroscopic Detection of Reverse Micelles in Supercritical Xenon. Figure 2 exhibits the ^{1}H NMR spectrum of a sample containing 50 mM AOT at 298 K and a xenon pressure of 15 MPa. The aqueous solution added to the AOT ($w_0 = 3$) contained 50 mM potassium phosphate buffer (pH 5.5) and 250 mM NaCl. On the basis of the chemical-shift values observed for AOT dissolved in methanol, the spectrum measured in supercritical xenon could be assigned (see Figure 2). The spectrum exhibits a number of intense signals attributed to CH_3 ($\delta = 0.9$ ppm), CH_2 ($\delta = 1.3$ ppm), CH_2-1′ ($\delta = 1.6$ ppm), CH-4/4′ ($\delta = 3.1$ ppm), CH_2-3 or 3′ ($\delta = 4.1$ ppm), and CH-1 ($\delta = 4.3$ ppm). Apart from these signals, another intense line at ca. 4 ppm could be observed and assigned to H_2O since this signal disappears from the spectrum if H_2O is replaced by D_2O. Note that the latter signal exhibits a shoulder at ca. 3.9 ppm, which does not disappear if H_2O is replaced by D_2O. This signal is assigned to be due to CH_2-3 or 3′ in addition to the signal at 4.1 ppm. The formation of reverse micelles in the supercritical xenon could be proven by two NMR experiments, namely, the determination of T_2 using CPMG experiments and by PFG experiments. Assuming the magnetic dipole−dipole interaction among ^{1}H nuclei to be the dominant source of transverse relaxation, T_2, of a CH_2 group caused by rotational diffusion of the reverse micelle is given by the equation[27]

$$\frac{1}{T_2} = q\left[\frac{3}{2}J(0) + \frac{5}{2}J(\omega_0) + J(2\omega_0)\right] \qquad (3)$$

with

$$q = \frac{3}{4}\left(\frac{\mu_0}{4\pi}\right)^2 \frac{\gamma^4\hbar^2}{r^6}$$

Here, γ denotes the gyromagnetic ratio of the spins I, μ_0 is the permeability of vacuum, $\hbar$ denotes the Planck constant divided by 2π, r is the distance to the neighboring nucleus, and ω_0 is the Larmor frequency of the considered nuclei. Other nuclei in the neighborhood of the considered CH_2 group are neglected within this estimation. Assuming isotropic rotational diffusion,

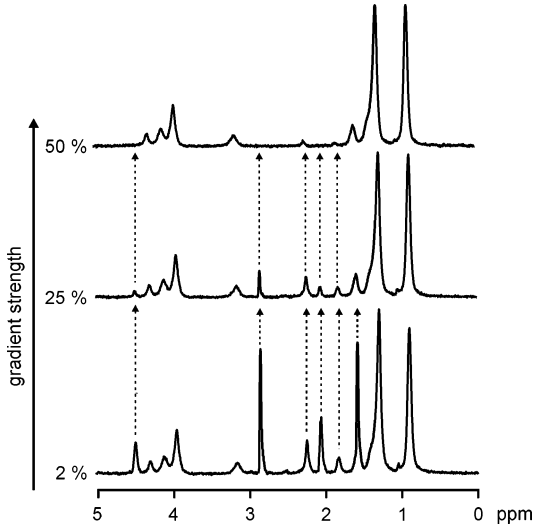

Figure 3. ^{1}H PFG NMR spectra of 50 mM AOT in supercritical xenon at a pressure of 15 MPa. Note that the sample preparation was identical to Figure 2 except for the salt concentration of the aqueous solution. The sample studied here was salt-free. Dotted lines indicate monomer signals. These signals are attenuated at increasing gradient strength. Signals due to reverse micelles persist due to the lower diffusion coefficient.

the spectral density function, $J(\omega,\tau_C)$, is defined by

$$J(\omega) = \frac{\frac{2}{5}\tau_C}{1 + \omega^2 {\tau_C}^2} \quad (4)$$

If the AOT molecules existed as monomers, T_2 values of the order of tens to hundreds of ms would be expected according to an estimation based on eqs 2−4. CPMG measurements on the sample shown in Figure 2, however, revealed a T_2 value of 6 ms for the signal at 1.3 ppm (CH_2 of AOT). This observation shows that the AOT molecules obviously form larger aggregates, namely, reverse micelles. The same is true for the signal at ca. 4 ppm (H_2O) indicating the incorporation of the water molecules into the reverse micelles. The diameter of the formed reverse micelles can at least roughly be estimated from the measured transverse and longitudinal relaxation times, T_2 (see eq 3) and T_1.[27] By assumption of a reverse micelle of spherical shape, their correlation time, τ_C, can be determined from the ratio $T_1/T_2 = \epsilon$ according to the equations

$$\tau_C = \frac{x^{1/2}}{\omega_0} \quad (5)$$

$$x = \frac{1}{24}[(16\epsilon - 37) + ((37 - 16\epsilon)^2 - 480(1 - \epsilon))^{1/2}] \quad (6)$$

The hydrodynamic radius, r, of the micelle is then readily calculated from eq 2. The relaxation times $T_1 = 810$ ms and $T_2 = 6$ ms measured for the 1.3-ppm signal (CH_2) at a xenon pressure of 15 MPa then result in a hydrodynamic radius of about 5 nm, i.e., a diameter of 10 nm for the reverse micelles.

The other striking evidence for the formation of reverse micelles arises from PFG experiments. Figure 3 exhibits ^{1}H PFG NMR spectra of reverse micelles ($w_0^{th} = 6$). In contrast to the spectrum shown in Figure 2, narrow additional signals appear which are indicated by the dotted lines. These signals must be ascribed to monomeric molecules (AOT and possibly water) since the diffusion coefficient is much higher than that measured for the above-described signals due to reverse micelles. At a gradient strength corresponding to 50% of the maximum value, the signals due to monomeric molecules are almost completely suppressed, while the signals of the reverse micelles are only slightly dampened. Note that the sample preparation was identical to the sample shown in Figure 2 except for the salt concentration. The water solution used for the sample shown in Figure 2 contained 50 mM potassium phosphate (pH 5.5) and 250 mM sodium chloride, while the sample studied in Figure 3 was free of salt. This demonstrates that the formation of reverse micelles is greatly facilitated by the addition of the described amount of salt to the aqueous solution used for the preparation of the samples. The time required for equilibration as well as the amount of monomeric molecules remaining in the samples is minimized at these concentrations. Therefore, all samples studied within the present paper were prepared correspondingly. It could, furthermore, be shown that the amount of monomeric molecules dissolved in the supercritical xenon drastically increases at xenon pressures below 10 MPa. All samples were therefore subjected to xenon pressures beyond 10 MPa.

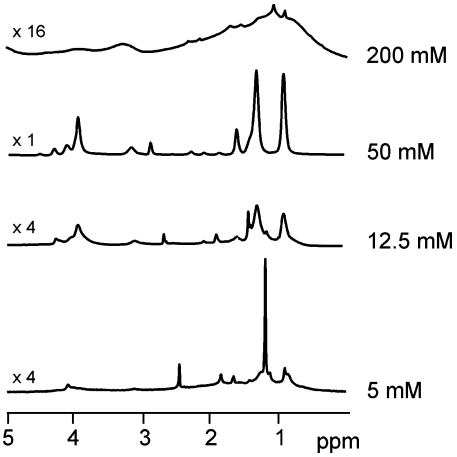

Figure 4. ^{1}H NMR spectra of reverse micelles in supercritical xenon (15 MPa) at various concentrations of AOT with $w_0^{th} = 6$.

Influence of AOT and H_2O Concentration upon the Formation of Reverse Micelles. We have studied the influence of AOT concentration upon the ^{1}H NMR spectra of reverse micelles (see Figure 4). Below a critical AOT concentration of 4 mM, reverse micelles could not be formed at $w_0^{th} = 6$ and 15 MPa xenon pressure. At 5 mM AOT, relatively strong signals due to monomers are still observed apart from the characteristic signals due to reverse micelles. For concentrations beyond ca. 20 mM AOT, reverse micelles are preferentially formed while the signals due to monomeric molecules almost disappear. At 200 mM AOT, the ^{1}H NMR signals become extremely broad indicating that the reorientation of the reverse micelles is slowed. This effect may be explained either by an increasing size of the micelles or by the interaction between neighboring micelles. AOT concentrations between 25 and 100 mM are the optimum (see also Figure 4).

As it was already mentioned in the Experimental Section, the real w_0 value within the reverse micelles was often observed to be lower than the theoretical value, w_0^{th}. A systematic study of this effect at an AOT concentration of 50 mM and 15 MPa xenon pressure is shown in Figure 5. For all samples, w_0 is considerably lower than w_0^{th}. A maximum real w_0 value of 3.6 could be observed at $w_0^{th} = 12$. At higher w_0^{th} values, the real w_0 drops down. Since the ^{1}H NMR spectra shown in Figure 5 exhibit only weak monomer signals, the formation of a separate

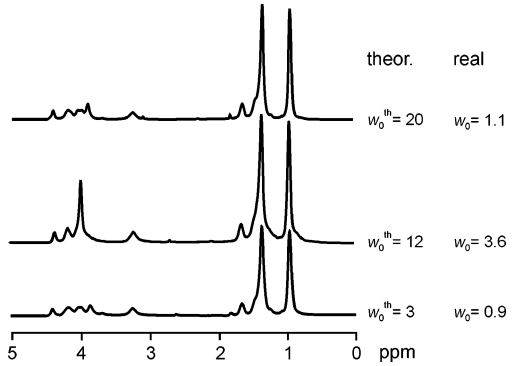

Figure 5. ^{1}H NMR spectra of reverse micelles formed by 50 mM AOT in supercritical xenon (15 MPa) at various values of w_0^{th}. The real w_0 values were determined as described in the Experimental Section.

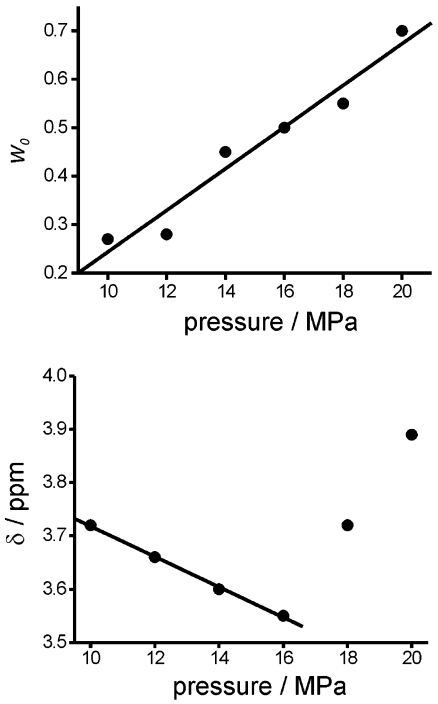

Figure 6. Top: Real w_0 value of reverse micelles formed by 50 mM AOT with $w_0^{th} = 1$ as a function of the applied xenon pressure. Bottom: ^{1}H NMR chemical shift, δ, of H_2O in reverse micelles (50 mM AOT, $w_0^{th} = 1$) as a function of the applied xenon pressure.

water phase outside the active volume of the receiver coil must be assumed. This water is located outside the receiver coil since the density of liquid water is lower than the density of xenon at the pressures applied in our experiments. The resulting buoyancy lifts the water to the top of the sample tube, i.e., outside the active volume of the receiver coil. A corresponding study at 60 MPa and with 50 mM AOT revealed a maximum real w_0 value of 8 at this pressure. The pressure dependence of w_0 is also demonstrated in Figure 6 for $w_0^{th} = 1$. A linear interdependence between the xenon pressure and w_0 inside the micelles is observed. Interestingly, the ^{1}H NMR chemical shift of the water molecules first decreases for increasing pressure. After passing through a minimum at ca. 16 MPa, it continuously increases. It is known from ^{1}H NMR studies of reverse micelles in liquid isooctane that the chemical shift, δ, of water inside the micelles continuously increases with increasing real w_0. This effect is explained by the exchange between water molecules at the water/surfactant interface and bulk water molecules within the water pool of the micelles. An increase of w_0 will then result

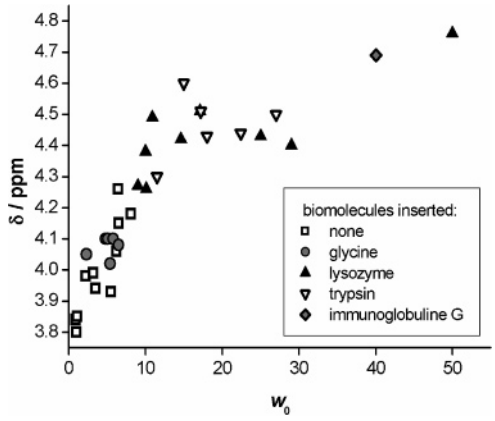

Figure 7. ^{1}H NMR chemical shift, δ, of H_2O in reverse micelles (50 mM AOT) as a function of the real w_0. To prepare reverse micelles with higher w_0 values, biomolecules had to be incorporated. The symbols corresponding to the different biomolecules inserted into the reverse micelles are explained in the inlet.

in a shift of δ toward the signal of bulk water at about 4.8 ppm. Apart from this well-known effect, however, reverse micelles in supercritical xenon exhibit a second effect: Increasing pressure obviously results in a decrease of δ which is the dominating effect below 16 MPa. This effect may be explained by a pressure dependence of the chemical shift for water molecules at the water/surfactant interface. If so, one could conclude that the increasing xenon pressure influences the interaction between the water molecules and the polar headgroups of the surfactant molecules. For higher pressures, that means for further increasing real w_0 inside the micelles, the above-described influence of w_0 dominates resulting in the observed increase of δ. Figure 7 shows the ^{1}H NMR chemical shift of water, δ, for w_0 values up to 50. These high values of w_0 could only be obtained for reverse micelles containing biomolecules. As it was described above, maximum w_0 values of ca. 8 could be observed for pure AOT/H_2O/Xe mixtures at 60 MPa. Although the composition of the samples studied in Figure 7 was, therefore, necessarily different, an obvious correlation between δ and w_0 could be observed in complete analogy to the behavior found for reverse micelles in liquid isooctane.[28] The data scattering in this correlation is likely to be due to the described variations of the experimental parameters (see also Figure 7). The chemical shift steadily increases from 3.8 ppm for $w_0 \approx 1$ up to about 4.8 ppm at $w_0 \approx 50$. The latter value corresponds to the chemical shift of bulk water.

Encapsulation of Biomolecules. The amino acid glycine was chosen as a model system for the insertion of small molecules into reverse micelles. Glycine is water soluble (3.37 mol/L)[29] and insoluble in supercritical xenon. The ^{1}H/^{13}C HSQC NMR spectrum shown in Figure 8 demonstrates the encapsulation of glycine in reverse micelles dissolved in supercritical xenon. Samples were prepared with 50 mM AOT, $w_0^{th} = 6$ at 250 mM NaCl and a glycine concentration of 1 mM. A control experiment was performed putting pure glycine in supercritical xenon. No signal due to glycine was observed at all. This observation proves that glycine is indeed insoluble in supercritical xenon, but it can be inserted into the water pool of reverse micelles. The uptake of biomolecules by reverse micelles in other solvents is well-known to be influenced by the effective charge of the biomolecules.[30] Therefore, the pH of the aqueous solution in which the glycine was dissolved was varied from 4 to 8. However, no changes of the amount of glycine taken up by the reverse micelles could be found.

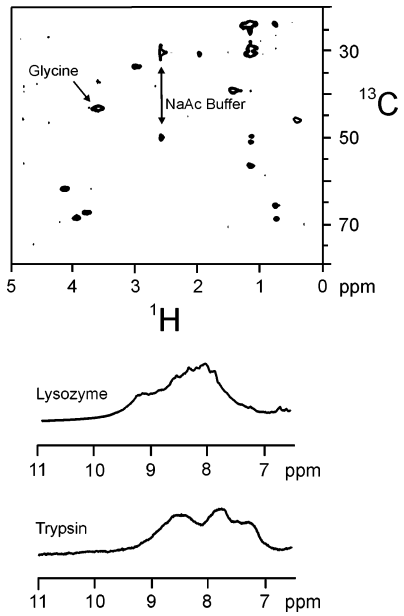

Figure 8. Top: ^{1}H/^{13}C HSQC NMR spectrum of reverse micelles containing glycine (50 mM AOT, $w_0^{th} = 6$, 1 mM glycine at 20 MPa). Cross-peaks due to glycine and sodium acetate buffer molecules are indicated. All unassigned peaks are due to the surfactant AOT. Bottom: ^{1}H NMR spectrum (H^N region) of 1 mg lysozyme and trypsin encapsulated in reverse micelles. Samples were prepared with 50 mM AOT and $w_0^{th} = 50$ at 35 MPa.

It is also possible to insert large biomolecules such as proteins into reverse micelles dissolved in supercritical xenon. This is demonstrated in Figure 8 (bottom) for the proteins lysozyme (14.3 kDa) and trypsin (23.8 kDa). Samples contained 1 mg of the corresponding protein and were prepared with $w_0^{th} = 50$. A minimum xenon pressure of 35 MPa was found to be necessary for protein encapsulation, otherwise the reverse micelles turned out to be unstable. The ^{1}H NMR spectra of lysozyme and trypsin in AOT/H_2O/Xe solutions clearly reveal protein signals in the H^N region. It is known for reverse micelles in liquid alkanes that protein encapsulation results in changes of the size and water content of reverse micelles.[30] As it was described above, the maximum w_0 value obtained in pure reverse micelles without encapsulated molecules was 8 at a xenon pressure of 60 MPa. For reverse micelles with encapsulated proteins, w_0 varied from 15 at 35 MPa to 50 at 60 MPa. That means that w_0 increases if proteins are encapsulated in the reverse micelles. The line widths of the AOT signals observed for these samples amount to ca. 50 Hz. For the encapsulated biomolecules, similar values are to be expected. This is obviously the reason for the low resolution in the one-dimensional ^{1}H NMR spectra of the proteins (see Figure 8, bottom).

Conclusion

Our results show the suitability of the NMR technique to investigate reverse micelles in supercritical fluids under high pressure. The ^{1}H NMR signals of reverse micelles in supercritical xenon could be identified and distinguished from the monomer signals. The formation of reverse micelles was studied as a function of various parameters and the optimum conditions for reverse micelle formation could be determined. It could be shown for the pure AOT/H_2O/Xe system that the real w_0 value exhibits an upper bound. This maximum real w_0 was found to be pressure dependent and amounts to ca. 8 for a xenon pressure of 60 MPa. Furthermore, encapsulation of biomolecules in reverse micelles dissolved in supercritical xenon is demonstrated for the first time. In contrast to the pure AOT/ H_2O/Xe system, real w_0 values up to ca. 50 were found for protein-containing reverse micelles.

Acknowledgment. Thanks are due to Professor Alexander Pines (Berkeley), Professor Hans Robert Kalbitzer (Regensburg), and Dr. Megan Spence (Zurich) for fruitful discussions and help in the initial state of the project. Furthermore, the authors wish to thank Ms. Ingrid Cuno for carefully proofreading the manuscript. Financial support by the Deutsche Forschungsgemeinschaft (Project Br 1278/9-1,2 and SFB 521, Project No. A6) is gratefully acknowledged.

References and Notes

(1) Arai, Y.; Sako, T.; Takebayashi, Y. *Supercritical Fluids*; Springer: Berlin, Heidelberg, New York, 2002.
(2) Ekwall, P. *J. Colloid Interface Sci.* **1969**, *29*, 16−26.
(3) Grandi, C.; Smith, E. R.; Luisi, P. L. *J. Biol. Chem.* **1981**, *256*, 837−843.
(4) Luisi, P. L. *Angew. Chem., Int. Ed. Engl.* **1985**, *24*, 439−528.
(5) Göklen, K. E.; Hatton, T. A. *Biotechnol. Prog.* **1985**, *1*, 69−74.
(6) Luisi, P. L.; Giomini, M.; Pileni, M. P.; Robinson, B. H. *Biochim. Biophys. Acta* **1988**, *947*, 209−246.
(7) Wand, A. J.; Ehrhardt, M. R.; Flynn, P. F. *Proc. Natl. Acad. Sci. U.S.A.* **1998**, *95*, 15299−15302.
(8) Babu, C. R.; Flynn, P. F.; Wand, A. J. *J. Biomol. NMR* **2003**, *25*, 313−323.
(9) Gaemers, S.; Elsevier, C. J.; Bax, A. *Chem. Phys. Lett.* **1999**, *301*, 138−144.
(10) Wu, W.-J.; Vidugiris, G.; Mooberry, E. S.; Westler, W.; Markley, J. L. *J. Magn. Reson.* **2003**, *164*, 84−91.
(11) Flynn, P. F. *Prog. Nucl. Magn. Reson. Spectrosc.* **2004**, *45*, 31−51.
(12) Peterson, R. W.; Anbalagan, K.; Tommos, C.; Wand, A. J. *J. Am. Chem. Soc.* **2004**, *126*, 9498−9499.
(13) Cavanagh, J.; Fairbrother, W. J.; Palmer, A. G., III; Skelton, N. J. *Protein NMR Spectroscopy*; Academic Press: San Diego, 1996.
(14) Pervushin, K.; Riek, R.; Wider, G.; Wüthrich, K. *Proc. Natl. Acad. Sci. U.S.A.* **1997**, *94*, 12366−12371.
(15) Pervushin, K.; Riek, R.; Wider, G.; Wüthrich, K. *J. Am. Chem. Soc.* **1998**, *120*, 6394−6400.
(16) Goto, M.; Ono, T.; Nakashio, F.; Hatton, T. A. *Biotechnol. Bioeng.* **1997**, *54*, 26−32.
(17) De, T. K.; Maitra, A. *Adv. Colloid Interface Sci.* **1995**, *59*, 95−193.
(18) Haake, M.; Goodson, B. M.; Laws, D.; Brunner, E.; Cyrier, M.; Havlin, R. H.; Pines, A. *Chem. Phys. Lett.* **1998**, *292*, 686−690.
(19) Leawoods, J. C.; Saam, B. T.; Conradi, M. S. *Chem. Phys. Lett.* **2000**, *327*, 359−364.
(20) Navon, G.; Song, Y.-Q.; Rõõm, T.; Appelt, S.; Taylor, R. E.; Pines, A. *Science* **1996**, *271*, 1848−1851.
(21) Fulton, J. L.; Blitz, J. P.; Tingey, J. M.; Smith, R. D. *J. Phys. Chem.* **1989**, *93*, 4198−4204.
(22) Smith, R. D.; Fulton, J. L.; Blitz, J. P.; Tingey, J. M. *J. Phys. Chem.* **1990**, *94*, 781−787.
(23) Baumer, D.; Fink, A.; Brunner, E. *Z. Phys. Chem.* **2003**, *217*, 289−293.
(24) Martin, C. A.; Magid, L. J. *J. Phys. Chem.* **1981**, *85*, 3938−3944.
(25) Altieri, A. S.; Hinton, D. P.; Byrd, R. A. *J. Am. Chem. Soc.* **1995**, *117*, 7566−7567.
(26) Bodenhausen, G.; Ruben, D. J. *Chem. Phys. Lett.* **1980**, *69*, 185−189.
(27) Abragam, A. *The Principles of Nuclear Magnetism*; Clarendon Press: Oxford, 1996.
(28) Wong, M.; Thomas, J. K.; Nowak, T. *J. Am. Chem. Soc.* **1977**, *99*, 4730−4736.
(29) Nozaki, Y.; Tanford, C. *J. Biol. Chem.* **1971**, *246*, 2211−2217.
(30) Luisi, P. L.; Magid, L. J. *Crit. Rev. Biochem.* **1986**, *20*, 409−474.